Bayesian Reliability and Performance Assessment for Multi-State Systems

Yu Liu, *Member, IEEE*, Peng Lin, Yan-Feng Li, and Hong-Zhong Huang, *Member, IEEE*

***Abstract*—This paper develops a Bayesian framework to assess the reliability and performance of multi-state systems (MSSs). An MSS consists of multiple multi-state components of which the degradation follows a Markov process. Due to the lack of sufficient data, and only vague knowledge from experts, the transition intensities of multi-state components between any pair of states and the state probabilities cannot be precisely estimated. The proposed Bayesian method can merge prior knowledge from experts' judgments with continuous and discontinuous inspection data to obtain posterior distributions of transition intensities. A simulation method embedded with the universal generating function (UGF) is developed to estimate the posterior state probabilities, the reliability, and the performance of the entire MSS. Two numerical experiments are presented to demonstrate the effectiveness of the proposed method.**

***Index Terms*—Bayesian estimation, continuous inspection data, discontinuous inspection data, multi-state component, multi-state system, reliability assessment.**

Abbreviations:

MSS	Multi-State System
UGF	Universal Generating Function
MCMC	Markov Chain Monte Carlo

Notation:

$g_{(l,i)}$	Performance capacity of component l at its state i.
$p^{l}_{(u,i)}(t)$	Probability of component l being at state i at time instant t if it is initially at state u at $t=0$.
$p_i(t)$	State probability of a system staying at state i at time t.
g_i	System performance capacity at state i.
$\lambda^{l}_{(i,j)}$	Transition intensity of component l from its state i to state j.
$l(data \mid \boldsymbol{\lambda}^{l})$	Likelihood function of transition intensities $\boldsymbol{\lambda}^{l}$.
$m_{(i,j)}$	Observed number of transitions from state i to state j via continuous inspection.
T_i	Total observed time of all the samples of a component sojourning at state i with continuous inspection.
m_i	Total observed number of transitions from state i via continuous inspection.
$m^{\Delta t_v}_{(i,j)}$	Observed number of all the samples of a component being inspected at state i in the last inspection and at state j after inspection interval Δt_v.

Manuscript received September 15, 2013; revised June 17, 2014; accepted August 11, 2014. Date of publication November 21, 2014; date of current version February 27, 2015. This work was supported by the National Natural Science Foundation of China under contract number 71101017 and the Specialized Research Fund for the Doctoral Program of Higher Education of China under contract number 20110185120014. Associate Editor: S. J. Bae.

The authors are with the School of Mechanical, Electronic, and Industrial Engineering, University of Electronic Science and Technology of China, Chengdu 611731, China (e-mail: yuliu@uestc.edu.cn; penglin1992@hotmail.com; yanfengli@uestc.edu.cn; hzhuang@uestc.edu.cn).

Color versions of one or more of the figures in this paper are available online at http://ieeexplore.ieee.org.

Digital Object Identifier 10.1109/TR.2014.2366292

I. Introduction

As more engineered systems are evolving to larger scale, more complexity, and higher precision, it is frequently observed that systems and components may manifest multiple states ranging from perfect, through deterioration, to complete failure [1]. Multi-state system (MSS) reliability theory, which is capable of characterizing the deterioration process of aging systems by introducing more than one intermediate state between perfectly working and completely failed states, has been recognized as a more effective tool to appropriately reveal hidden stochastic behaviors of advanced engineering systems [2]. Many engineering systems can be treated as an MSS in practice, such as manufacturing systems [3], power generating systems [4], communication systems [5], and municipal infrastructure [6]. In these types of multi-state systems, both the system and its components can perform their intended tasks with more than two discrete states distinguished by levels of efficiency or performance capacity. Various methods, like the extended decision diagram-based method [7], the stochastic process [8], the universal generating function (UGF) [9], the recursive algorithm [10], and simulation-based methods [5], have been proposed to assess the reliability and performance of MSSs.

It is worth mentioning that nearly all the reported studies on MSS reliability assessment are based on two critical assumptions: 1) the transition intensities between any pair of states are known, and 2) the state probabilistic distributions can be estimated precisely from sampling data. The emphasis of existing works lies in modeling MSSs that possess complicated deteriorating behaviors, improving computational efficiency for reliability evaluation, and optimizing the system configuration to achieve better reliability performance [1], [2]. In fact, estimation or inference of model parameters is a preceding task before reliability evaluation and optimization can be carried out. However, less attention has been paid to parameter estimation in the context of MSSs. Lisnianski *et al.* [14] introduce the point estimation of transition intensities of a multi-state power generating unit by defining a special Markov chain embedded in the observed capacity process. However, due to the lack of sufficient

data, accurate estimation of transition intensities and state distributions turns out to be a challenging task [11], [12]. The aforementioned method can only yield the point estimates of transition intensities, yet is unable to quantify the uncertainty or compute the confidence bounds of the estimates. Such a limitation may lead to a large estimation error if the results are overestimated or underestimated, especially in the case of sparse or limited data. Most recently, fuzzy numbers [11],[12], [15], interval values [16], and belief functions [17] are adopted to quantify the uncertainty of state probabilities and transition intensities when precise knowledge or sufficient data are not available. Though these methods can provide confidence bounds to measure the uncertainty of estimated parameter values, such as state probabilities and transition intensities, such uncertainty cannot be sequentially characterized and reduced by collecting more data. From a statistical point of view, the estimation should asymptotically approach the true values, though unknown, as the amount of observations increases.

To address the aforementioned issue, this paper presents a Bayesian framework to assess the reliability and performance of multi-state systems. The Bayesian approach, which treats the parameter estimate as a random variable, has been used in different engineering fields where data can be progressively accumulated over time [18]. This method enables reliability engineers to systematically synthesize the subjective information from experts and intuitive judgments with actual observed data, thereby obtaining a balanced estimate. That is, the estimate is updated as more information and data become available [19]. As a key advantage over other methods (e.g., fuzzy sets, interval values), the Bayesian approach is able to quantify the uncertainty arising from limited data. Many practical problems under the context of binary-state systems have been successfully solved under classic Bayesian reliability analysis [20], [21]. Bayesian reliability assessment for multi-state components and systems is, however, rarely reported in literature, which motivates the development of this work.

In this paper, we propose a Bayesian framework for reliability and performance assessment of multi-state systems. The likelihood functions in Bayesian parameter estimation of multi-state components are derived in two common cases, namely components are inspected continuously, and discontinuously. The posterior state probability for the system is computed via Monte Carlo simulation coupled with the UGF technique. The application of the proposed method is demonstrated via two numerical examples.

The remainder of the paper is organized as follows. The continuous-time Markov model which characterizes deterioration processes of multi-state components is briefly reviewed in Section II. The Bayesian estimation of transition intensities of multi-state components with continuous inspection data and discontinuous inspection data are respectively developed in Section III. Reliability function, state probabilities, and many other quantities of interests of multi-state systems are assessed based on the posterior distributions of transition intensities of multi-state components in Section IV. In Section V, two numerical examples are exemplified to illustrate the effectiveness and accuracy of the proposed method, and it is followed by a brief conclusion and some remarks in Section VI.

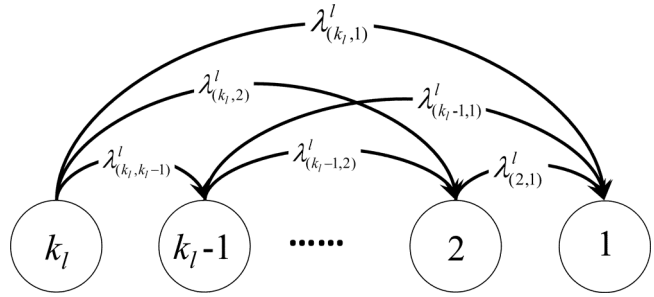

Fig. 1. The state-space diagram for multi-state component l without any repair.

II. Markov Model for Evaluating State Probabilities of Multi-State Components

To analyze the behavior of a MSS, one has to start with characterizing the stochastic behavior of its components. Any multi-state component l in an MSS has k_l different states each corresponding to a distinct performance capacity which is represented by the set $\mathbf{g}_l = \{g_{(l,1)}, g_{(l,2)}, \ldots, g_{(l,k_l)}\}$, where $g_{(l,i)} \geq 0$ is the performance capacity of component l at state i, $i \in \{1, 2, \ldots, k_l\}$. The performance capacity $G_l(t)$ of component l at any instant $t \geq 0$ is a random quantity, taking values from $\mathbf{g}_l$, i.e., $G_l(t) \in \mathbf{g}_l$. Therefore, during a time interval $[0, T]$, the performance capacity of component l is defined as a stochastic process. The probabilities associated with different states of component l at time instant t given the condition that the component degrades initially from state $u (u > 1)$ are denoted by the set $\mathbf{p}^l_u(t) = \{p^l_{(u,1)}(t), p^l_{(u,2)}(t), \ldots, p^l_{(u,k_l)}(t)\}$, where $p^l_{(u,i)}(t)$ represents the probability that $G_l(t) = g_{(l,i)}$. The state probabilities satisfy the condition $\sum_{i=1}^{k_l} p^l_{(u,i)}(t) = 1$ because the components' states at any time instant t constitute a complete set of mutually exclusive events.

With a memoryless assumption that the probability of a future state of component l is s-independent of its previous state, the stochastic behavior of multi-state components can be characterized by a Markov process. In our study, we investigate the case where the deterioration of multi-state components follows a homogenous continuous-time Markov process. Many engineering systems possess a multi-state nature, including manufacturing systems [2], power systems [4], and flow transmission systems [22]. These types of systems can be characterized by a homogenous continuous-time Markov model. The proposed method can be further extended to more general cases such as non-homogenous continuous-time Markov models and semi-Markov models.

An example of the state-space diagram of multi-state component l without considering repair activities is depicted in Fig. 1. The corresponding Kolmogorov differential equations for component l can be expressed as

$$\frac{dp^l_{(u,i)}(t)}{dt} = \sum_{j=i+1}^{k_l} p^l_{(u,j)}(t)\lambda^l_{(j,i)} - p^l_{(u,i)}(t)\sum_{j=i}^{i-1}\lambda^l_{(i,j)}, \quad (1)$$

where the initial conditions are $p^l_{(u,u)}(0) = 1$, and $p^l_{(u,i)}(0) = 0 (i \neq u)$. By solving the differential equations, one can get the state probability $p^l_{(u,i)}(t)$ as a function of time [2].

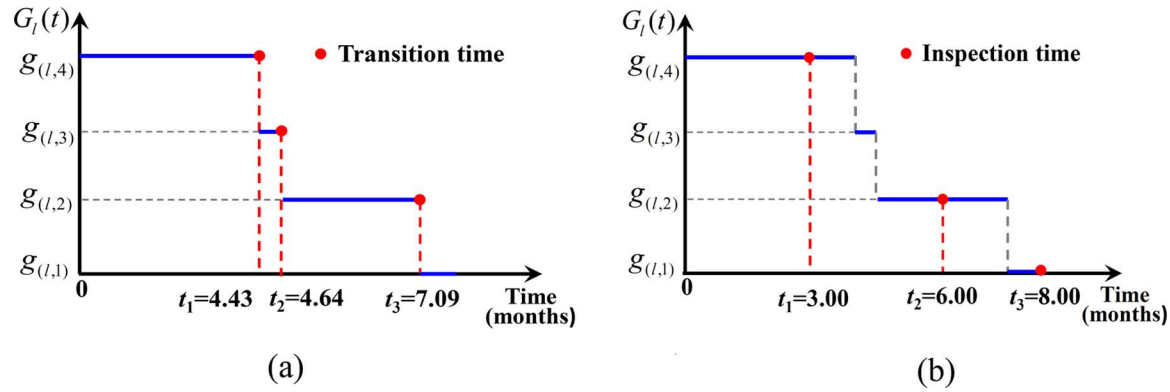

Fig. 2. Observation data from continuous and discontinuous inspections. (a) Data collected for sample #10 under continuous inspection. (b) Data collected for sample #10 under discontinuous inspection.

TABLE I
CONTINUOUS INSPECTION DATA OF 14 SAMPLES *

Sample#	Observed data	Sample#	Observed data
1	0 4.81 7.47 8.85 4 3 2 1	8	0 0.87 1.73 4 3 1
2	0 1.63 7.89 4 2 1	9	0 0.61 2.41 2.88 4 3 2 1
3	0 2.49 3.50 4 2 1	10	0 4.43 4.64 7.09 4 3 2 1
4	0 0.43 1.32 4 2 1	11	0 1.49 3.13 4 3 1
5	0 5.56 7.40 9.41 4 3 2 1	12	0 0.03 7.52 4 2 1
6	0 2.20 3.49 4 2 1	13	0 7.37 10.04 10.94 4 3 2 1
7	0 0.28 1.43 4 2 1	14	0 0.70 4 1

*Note: The first row of each sample is the exact transition times (months), and the second row of each sample is the state which the sample transited to.

III. BAYESIAN ESTIMATION OF TRANSITION INTENSITIES OF MULTI-STATE COMPONENTS

Based on the Bayes' theorem, the posterior distribution of unknown parameters $\boldsymbol{\lambda}^l$ (i.e., transition intensities) can be estimated by

$$f^{post}(\boldsymbol{\lambda}^l \mid data) = \frac{l(data \mid \boldsymbol{\lambda}^l) f^{prior}(\boldsymbol{\lambda}_l)}{\int l(data \mid \boldsymbol{\lambda}^l) f^{prior}(\boldsymbol{\lambda}^l) \mathrm{d}\boldsymbol{\lambda}^l}, \quad (2)$$

where $f^{prior}(\boldsymbol{\lambda}^l)$ is the prior distribution of unknown parameters $\boldsymbol{\lambda}^l$ given by experts' subjective judgments, and $f^{post}(\boldsymbol{\lambda}^l \mid data)$ is the posterior distribution of $\boldsymbol{\lambda}^l$ after combining the observed data.

To conduct the Bayesian estimation of transition intensities of multi-state components, one has to first construct a likelihood function to estimate the unknown parameter $\boldsymbol{\lambda}^l$ (i.e., transition intensities) based on observed data. Together with prior information of unknown parameters, the posterior distributions $\boldsymbol{\lambda}^l$ of can be readily estimated via (2).

In the ensuing subsections, two cases, i.e., continuous inspection data and discontinuous inspection data, are considered as they are the most common practices in real-world applications.

A. Estimation With Continuous Inspection Data

In this case, the exact transition times of multi-state components from one state to another are recorded. Put another way, components are continuously inspected, and any event associated with state transition is tracked. Examples of such continuous inspection data of 14 pieces of identical multi-state components are tabulated in Table I, the deterioration process and transition times of sample #10 are delineated in Fig. 2(a). As seen from Fig. 2(a), sample #10 of the studied component transited to state 3 after sojourning at state 4 for 4.43 months, and then transited to state 2 at 4.64 months, and eventually entered the worst state 1 at 7.09 months.

To construct the likelihood function, one needs to rearrange the data set. Let $m_{(i,j)}(i > j, i \in \{2,3,\ldots,k_l\}, j \in \{1,2,\ldots,k_l\})$ denote the number of transitions from state i to state j among all the observed data, and $T_i(i \in \{2,3,\ldots,k_l\})$ denote the total time that components are sojourning at state i. The data in Table I can be therefore converted into the format shown in Table II.

Let $m_i(i = 2,3,\ldots,n)$ be the total number of transitions from state i, i.e., $m_i = \sum_{j=1}^{i-1} m_{(i,j)}$. Under the assumption that the deterioration of multi-state component l follows a homogenous continuous-time Markov model, m_i follows a

TABLE II
REARRANGED CONTINUOUS INSPECTION DATA OF 14 SAMPLES

Initial state i of a transition	Total sojourning time(months) T_i	Total number m_i	Destination state j of a transition		
			$j=3$	$j=2$	$j=1$
			$m_{(i,3)}$	$m_{(i,2)}$	$m_{(i,1)}$
$i=4$	32.90	14	7	6	1
$i=3$	11.68	7	—	5	2
$i=2$	25.29	11	—	—	11

Poisson process with the parameter equal to $\lambda^l_{(i,i)} \cdot T_i$, i.e., $m_i \sim \text{Poisson}(\lambda^l_{(i,i)} \cdot T_i)$. The corresponding probability density function, denoted as f_1, can be expressed as

$$f_1(m_i \mid \lambda^l_{(i,i)}.T_i) = \frac{(\lambda^l_{(i,i)}.T_i)^{m_i}}{m_i!} e^{-\lambda^l_{(i,i)} \cdot T_i}, \tag{3}$$

where $\lambda^l_{(i,i)} (i \in \{2,3,\ldots,k_l\})$ is the intensity of leaving state i, and one has $\lambda^l_{(i,i)} = \sum_{j=1}^{i-1} \lambda^l_{(i,j)}$.

If a transition at state i occurs, then the conditional probability $q^l_{(i,j)} (i > j, i \in \{2,3,\ldots,k_1\}, j \in \{1,2,\ldots,k_l - 1\})$ that the transition is from state i to state j is given by

$$q^l_{(i,j)} = \frac{\lambda^l_{(i,j)}}{\lambda^l_{(i,i)}}. \tag{4}$$

With the assumption that the multi-state component deteriorates with a homogenous continuous-time Markov pattern, the set of quantities $(m_{(i,1)}, m_{(i,2)}, \ldots, m_{(i,i-1)}) (i \in \{2,3,\ldots,k_l\})$ follows the multinomial distribution with parameters m_i and $\mathbf{q}^l_i = (q^l_{(i,1)}, q^l_{(i,2)}, \ldots, q_{(i,i-l)})$. The corresponding multinomial probability mass function, denoted as f_2, is written as

$$\begin{aligned} &f_2(m_{(i,1)}, \ldots, m_{(i,i-1)} | \mathbf{q}^l_i, m_i) \\ &= \frac{m_i!}{\prod_{j=1}^{i-1} m_{(i,j)}!} {q^l_{(i,1)}}^{m_{(i,1)}} \cdots {q^l_{(i,i-1)}}^{m_{(i,i-1)}}. \end{aligned} \tag{5}$$

Thus, the likelihood function is the product of the density functions of the Poisson distributions, i.e., (3), and the multinomial probability mass functions, i.e., (5), for all states, and it yields an expression as shown in (6) at the bottom of the page, where $\boldsymbol{\lambda}^l$ is the matrix containing all the transition intensities between any pair of states.

The prior information for the unknown parameters $\boldsymbol{\lambda}^l$ needs to be specified under the Bayesian estimation framework. The prior distribution for $\lambda^l_{(i,j)}$ could be chosen among the distributions of Gamma, Beta, and other types, depending on the prior knowledge or experts' subjective adjustments [18]. Note that the prior distribution cannot be specified arbitrarily, because the prior distribution has a significant impact on the posterior distribution, especially when the amount of observed data is limited. Several effective methods have been proposed to determine priori distributions, such as non-informative priors, conjugate priors, Jeffreys' priors, empirical Bayesian priors, maximum entropy priors, bootstrap priors, random weight priors, and probability encoding methods [18], [23].

B. Estimation With Discontinuous Inspection Data

It is oftentimes impossible and unaffordable to continuously inspect multi-state components in a system to get continuous inspection data that exactly capture the transition time. In most cases, multi-state components are inspected periodically or randomly, and only the state of components at each inspection point and the time interval between two adjacent inspections are recorded. The collected data cannot directly reveal how long the component resides in each state, or the exact transition path through which the component degrades from the last observed state to the current observed state. Compared to the continuous inspection, the discontinuous inspection data are more general and common in practical problems. A similar issue is encountered in the healthcare service industry, as reported in [24]. Examples of such observed data are tabulated in Table III, where the 14 samples listed in Table I are inspected with different time intervals. The inspection times of sample #10 are depicted in Fig. 2(b). For instance, sample #10 was observed at state 4 at $t = 3$ months, and at state 2 at $t = 6$ months. There is no information about how long sample #10 has been staying at state 4, and whether it moved from state 4 to state 3 and then to state 2, or directly transited from state 4 to state 2.

To conduct Bayesian estimation for this case, the likelihood should be constructed in advance. Under the assumption that a component's deterioration follows a homogenous continuous-time Markov model, the likelihood of the observed data of any individual component is *s*-dependent on the observed states of the component in the last inspection, regardless of its previous states sojourning before the last inspection. If the component is observed at state i in the last inspection, which can be regarded as the initial state of this inspection, the probability of the component being at state $j (j \in \{1,2,\ldots,i\})$ after Δt is denoted as $p^l_{(i,j)}(\Delta t)$, where Δt is the time interval between two adjacent inspections. $p^l_{(i,j)}(\Delta t)$ is a function of the inspection interval Δt and the component's transition intensities $\boldsymbol{\lambda}^l$, and it

$$l\left(data|\boldsymbol{\lambda}^l\right) = \prod_{i=2}^{k_l} \left(\frac{(\lambda^l_{(i,i)} \cdot Ti)^{m_i}}{m_i!} e^{-\lambda^l_{(i,i)} \cdot Ti} \cdot \frac{m_i!}{\prod_{j=1}^{i-1} m_{(i,j)}!} {q^l_{(i,1)}}^{m_{(i,1)}} \cdots {q^l_{(i,i-1)}}^{m_{(i,i-1)}} \right) \tag{6}$$

TABLE III
DISCONTINUOUS INSPECTION DATA OF 14 SAMPLES *

Sample#	Observed data	Sample#	Observed data
1	0 3 5 7 10	8	0 2
	4 4 3 3 1		4 1
2	0 2 5 7 9	9	0 2 4
	4 2 2 2 1		4 3 1
3	0 4	10	0 3 6 8
	4 1		4 4 2 1
4	0 3	11	0 3 5
	4 1		4 3 1
5	0 4 7 9 12	12	0 2 4 7 9
	4 4 3 2 1		4 2 2 2 1
6	0 2 5	13	0 4 8 11
	4 4 1		4 4 3 1
7	0 3	14	0 3
	4 1		4 1

*Note: The first row of each sample is the inspection times (months), and the second row of each sample is the states observed at inspection points.

can be computed by (1). Hence, all the observations with the same observed state in the last inspection and the same time interval Δt between two adjacent inspections can be regarded as repeated s-independent trials, and characterized by a multinomial distribution.

Let $m_{(i,j)}^{\Delta t}$ denote the number of inspections in which a sample is observed at state i in the last inspection, and at state j after an inspection interval Δt. One has $m_i^{\Delta t} = \sum_{j=1}^{i} m_{(i,j)}^{\Delta t}$. Notice that $m_{(i,i)}^{\Delta t} (i \in \{2,3,\ldots,k_l\})$ is a part of $m_i^{\Delta t}$, and it corresponds to the case where a component is observed in the same state i in two consecutive inspections with a time interval Δt. The set of quantities $(m_{(i,1)}^{\Delta t}, m_{(i,2)}^{\Delta t}, \ldots, m_{i,i}^{\Delta t})$ follows a multinomial distribution with parameters $m_i^{\Delta t}$ and $\mathbf{p}_i^l(\Delta t) = (p_{(i,1)}^l(\Delta t), p_{(i,2)}^l(\Delta t), \ldots, p_{(i,i)}^l(\Delta t))$. The corresponding multinomial probability mass function, denoted as f_3, is written as

$$f_3(m_{(i,1)}^{\Delta t}, m_{(i,2)}^{\Delta t}, \ldots, m_{(i,i)}^{\Delta t} \mid \mathbf{p}_i^l(\Delta t), m_i^{\Delta t}) = \frac{m_i^{\Delta t}!}{\prod_{j=1}^{i} m_{(i,j)}^{\Delta t}!} p_{(i,1)}^l(\Delta t)^{m_{(i,1)}^{\Delta t}} p_{(i,2)}^l(\Delta t)^{m_{(i,2)}^{\Delta t}} \cdots p_{(i,i)}^l(\Delta t)^{m_{(i,i)}^{\Delta t}}. \tag{7}$$

Nevertheless, random inspections are oftentimes implemented rather than periodical ones. In such cases, there is more than one distinct time interval between two adjacent inspections, like the one shown in Table III. To generalize this scenario, a vector $\Delta\mathbf{t} = (\Delta t_1, \Delta t_2, \ldots \Delta t_n)(n \in \{1,2,\ldots\})$ with finite time intervals is used to represent distinct time intervals between two adjacent inspections in the cases of non-periodical inspections. To derive the likelihood function containing all the observed data, the original data has to be rearranged according to $\Delta\mathbf{t}$. For every $\Delta t_v (v \in \{1,2,\ldots,n\})$ within $\Delta\mathbf{t}$, one needs to get $m_i^{\Delta t_v} (i \in \{2,3,\ldots,k_l\})$ and $m_{(i,j)}^{\Delta t_v} (j \le i \in \{2,3,\ldots,k_l,\ j \in \{1,2,\ldots,k_l\})$ which can be counted from original data. For example, in Table III, there are three distinct time intervals between two adjacent inspections, i.e., 2 months, 3 months, and 4 months. Thus, one has $\Delta\mathbf{t} = (\Delta t_1 = 2, \Delta t_2 = 3, \Delta t_3 = 4)$ months. The data in Table III can be therefore converted to the form shown in Table IV. By rearranging the observed data, one can get the values of $(m_{(i,1)}^{\Delta t_v}, m_{(i,2)}^{\Delta t_v}, \ldots, m_{(i,i)}^{\Delta t_v})$ for each distinct inspection interval. Hence, the likelihood of all the observed data with the same inspection interval Δt_v but different observed states in the last inspection can be written as shown in (8) at the bottom of the page.

The likelihood of all the observed data can be derived by multiplying the likelihoods of all Δt_v, and written as shown in (9) at the bottom of the page.

$$\prod_{i=2}^{k_l} f_3\left(m_{(i,1)}^{\Delta t_v}, m_{(i,2)}^{\Delta t_v}, \ldots, m_{(i,i)}^{\Delta t_v} \mid \mathbf{p}_i^l(\Delta t_v), m_i^{\Delta t_v}\right) = \prod_{i=2}^{k_l} \left(\frac{m_i^{\Delta t_v}!}{\prod_{j=1}^{i} m_{(i,j)}^{\Delta t_v}!} p_{(i,1)}^l(\Delta t_v)^{m_{(i,1)}^{\Delta t_v}} p_{(i,2)}^l(\Delta t_v)^{m_{(i,2)}^{\Delta t_v}} \cdots p_{(i,i)}^l(\Delta t_v)^{m_{(i,i)}^{\Delta t_v}} \right) \tag{8}$$

$$l(data|\boldsymbol{\lambda}^l) = \prod_{v=1}^{n} \left(\prod_{i=2}^{k_l} \left(\frac{m_i^{\Delta t_v}!}{\prod_{j=1}^{i} m_{(i,j)}^{\Delta t_v}!} p_{(i,1)}^l(\Delta t_v)^{m_{(i,1)}^{\Delta t_v}} p_{(i,2)}^l(\Delta t_v)^{m_{(i,2)}^{\Delta t_v}} \cdots p_{(i,i)}^l(\Delta t_v)^{m_{(i,i)}^{\Delta t_v}} \right) \right) \tag{9}$$

TABLE IV
REARRANGED DISCONTINUOUS INSPECTION DATA OF 14 SAMPLES

State i observed in the last inspection	Inspection interval $\Delta t_1 = 2$ months				
	State j observed in adjacent inspection				
		$j=4$	$j=3$	$j=2$	$j=1$
	$m_i^{\Delta t_1}$	$m_{(i,4)}^{\Delta t_1}$	$m_{(i,3)}^{\Delta t_1}$	$m_{(i,2)}^{\Delta t_1}$	$m_{(i,1)}^{\Delta t_1}$
$i=4$	6	1	2	2	1
$i=3$	4	—	1	1	2
$i=2$	5	—	—	2	3
State i observed in the last inspection	Inspection interval $\Delta t_2 = 3$ months				
	State j observed in adjacent inspection				
		$j=4$	$j=3$	$j=2$	$j=1$
	$m_i^{\Delta t_2}$	$m_{(i,4)}^{\Delta t_2}$	$m_{(i,3)}^{\Delta t_2}$	$m_{(i,2)}^{\Delta t_2}$	$m_{(i,1)}^{\Delta t_2}$
$i=4$	9	2	2	1	4
$i=3$	2	—	0	0	2
$i=2$	3	—	—	2	1
State i observed in the last inspection	Inspection interval $\Delta t_3 = 4$ months				
	State j observed in adjacent inspection				
		$j=4$	$j=3$	$j=2$	$j=1$
	$m_i^{\Delta t_3}$	$m_{(i,4)}^{\Delta t_3}$	$m_{(i,3)}^{\Delta t_3}$	$m_{(i,2)}^{\Delta t_3}$	$m_{(i,1)}^{\Delta t_3}$
$i=4$	4	2	1	0	1
$i=3$	0	—	0	0	0
$i=2$	0	—	—	0	0

By substituting (9) into the Bayesian formula (2), together with the prior distribution, one can obtain the posterior distributions of the unknown transition intensity estimates.

Note that, if there is no analytical solution to the posterior distributions of transition intensities, then the Markov Chain Monte Carlo (MCMC) method as an alternative can be used to generate a posterior distribution via simulation. The specific MCMC method used in our study is the Gibbs Sampling method, which samples one of the transition intensities from its conditional posterior distribution with the remaining transition intensities fixed at their current values. After an appropriate burn-in period of simulations, the samples of transition intensities produced by the Gibbs Sampling method can represent samples drawn from the posterior distributions of transition intensities. The details of the MCMC method are available in [20], [21], and it can be readily implemented via software, like OpenBUGS and WinBUGS [25]. The exemplified scripts of estimating posterior transition intensities for a three-state component with continuous, and discontinuous inspection data via the MCMC in the WinBUGS are given in the Appendix.

IV. RELIABILITY AND PERFORMANCE ASSESSMENT FOR MSS

The system performance distribution (also called state distribution) at any time instant can be determined based on its component state distribution along with the physical structure of the system [2]. By using the UGF [2], [9], the state distribution of a multi-state component can be expressed by a polynomial form as $u_l(z,t) = \sum_{i=1}^{k_l} p_{(u,i)}^l(t) z^{g(l,i)}$, where $p_{(u,i)}^l(t)$ computed by (1) is a function of transition intensities of component l.

Likewise, the performance distribution of an MSS can be written in the same UGF fashion as $U_S(z,t) = \sum_{i=1}^{N_S} p_i(t) z^{g_i}$, where $p_i(t)$ denotes the probability of a system staying at state i at time instant t, and it is a function of component state probabilities, i.e., $p_{(u,i)}^l(t)$; g_i is the corresponding performance capacity of system state i; N_S is the total number of system states. The UGF of the system can be recursively determined by UGFs of components via composition operators; see more details in [2], [9].

The reliability of the MSS in question is defined as the probability that the system's performance capacity is not less than the user demand W. If the user demand W is a random quantity with H possible discrete values, denoted as $W = \{w_1, \ldots, w_H\}$, and the corresponding probability mass function $\Pr\{W = w_i\} = q_i$, the system reliability function is formulated as

$$R(t) = \sum_{i=1}^{H} q_i \sum_{j=1}^{N_S} p_j(t) \cdot 1(g_j - w_i \geq 0), \tag{10}$$

where $1(\cdot)$ is a unity function, i.e., $1(\text{TRUE}) = 1$, and $1(\text{FALSE}) = 0$. The MSS instantaneous expected performance capacity at any time instant can be computed by

$$E(t) = \sum_{i=1}^{N_S} p_i(t) \cdot g_i. \tag{11}$$

Unlike existing works where transition intensities of multi-state components are assumed to be precisely known

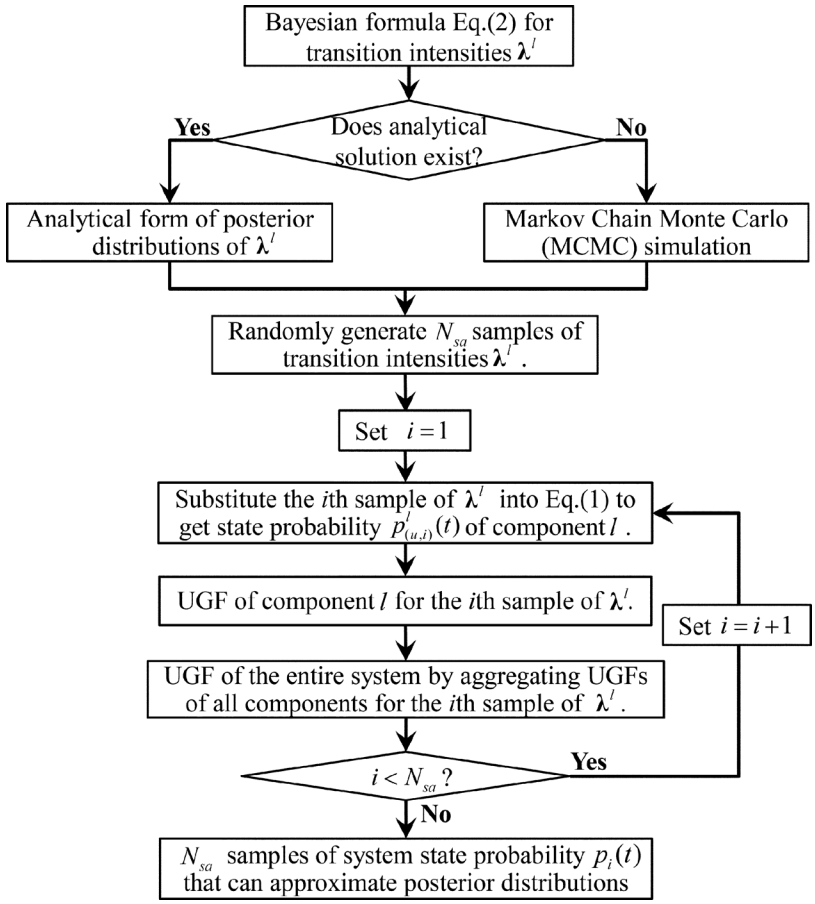

Fig. 3. The flowchart of generating the posterior distributions of system state probabilities via a simulation way.

or represented by crisp values (i.e., point estimation), in our study, transition intensities are estimated from both experts' prior knowledge and observed data. The estimated transition intensities of component l from the proposed Bayesian framework is characterized by the posterior distribution denoted as $f^{post}(\boldsymbol{\lambda}^l|data)$. Hence, for any time instant t, the probability of multi-state component l staying at state i is therefore a random quantity as well, and can be computed by substituting the posterior distributions of $\boldsymbol{\lambda}^l$ into (1). Moreover, the probability of system sojourning at state i at any time instant t is also a random quantity as it is a function of component state probabilities. Computing system state probabilities with the posterior distribution of transition intensities $\boldsymbol{\lambda}^l$ can be essentially viewed as an uncertainty propagation problem; that is, the estimation uncertainties of transition intensities $\boldsymbol{\lambda}^l$ will be eventually propagated to the system state level and other quantities of interests. Nevertheless, it is a challenging task to estimate the posterior distributions of these quantities of interests (e.g., system state probabilities, system reliability function, etc.) analytically due to nonlinearity between the transition intensities and these quantities. To overcome this issue, an alternative method (shown in Fig. 3) is developed in this work to approximate the posterior distributions of system state probabilities via simulation.

According to Fig. 3, N_{sa} samples of transition intensities $\boldsymbol{\lambda}^l$ for each component are randomly generated per the analytical expression of the posterior distribution (if its analytical solution exists by solving (2)) or the MCMC simulation, where N_{sa} is a pre-specified value in a range of $1000 \sim 5000$ representing the number of samples to be produced to approximate the posterior distribution. The state distribution of component l with respect to the ith sample of transition intensities $\boldsymbol{\lambda}^l$ can be obtained by solving (1). By aggregating the UGFs of all components for the ith sample of transition intensities $\boldsymbol{\lambda}^l$, one can get the UGF and the state distribution (i.e., $p_i(t)$) of the entire system with respect to the ith sample of transition intensities $\boldsymbol{\lambda}^l$ of all components. The posterior distributions of system state probabilities at any time t can be approximated by fitting all the N_{sa} samples of system state probability $p_i(t)$ with either a parametric distribution (e.g., normal, Weibull) or non-parametric distribution (e.g., the empirical distribution).

Because the state probability of components is a set of random quantities, the posterior system state probabilities are random quantities as well. Any pair of system state probabilities at any time t may be s-dependent if they share the same transition intensities from s-identical components. In addition, if an MSS contains more than one copy of the same type of component (also called repeated component in [26]), each sample of transition intensities randomly generated from posterior distributions should be simultaneously substituted into the UGFs for all the repeated components because these repeated components share the same reliability estimate [26].

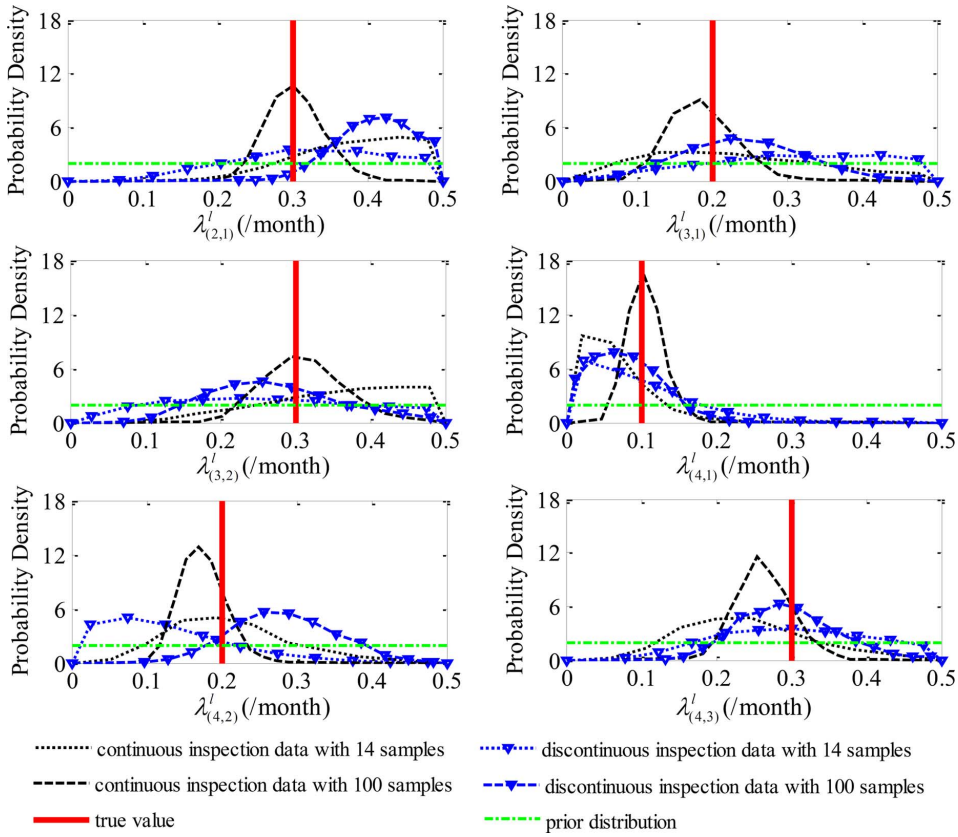

Fig. 4. Posterior distributions of λ^l for continuous inspection data and discontinuous inspection data.

TABLE V
POSTERIOR SUMMARIES OF λ^l FOR CONTINUOUS INSPECTION DATA AND DISCONTINUOUS INSPECTION DATA *

	Continuous inspection data			Discontinuous inspection data		
	Mean	Std	95% CB	Mean	Std	95% CB
$\lambda^l_{(2,1)}$	0.385	0.074	(0.228,0.494)	0.326	0.099	(0.131,0.489)
$\lambda^l_{(3,1)}$	0.229	0.113	(0.049,0.465)	0.308	0.116	(0.075,0.490)
$\lambda^l_{(3,2)}$	0.359	0.094	(0.157,0.493)	0.260	0.125	(0.044,0.485)
$\lambda^l_{(4,1)}$	0.061	0.043	(0.008,0.169)	0.092	0.071	(0.004,0.269)
$\lambda^l_{(4,2)}$	0.213	0.080	(0.085,0.402)	0.124	0.087	(0.007,0.333)
$\lambda^l_{(4,3)}$	0.241	0.082	(0.107,0.424)	0.305	0.097	(0.127,0.482)

*Std-Standard Deviation; CB-Confidence Bound.

V. ILLUSTRATIVE EXAMPLES

Two illustrative examples are presented in this section to demonstrate the implementation of the proposed method. The first example is used to illustrate the effectiveness of the proposed Bayesian method in terms of transition intensity estimation for a single component. In the second example, reliability and performance assessment for a multi-state power generation system will be conducted.

A. A Single Power Generator

The studied generator is a multi-state component with four possible performance capacities. The performance capacities with respect to each state are $g_{(l,4)} = 10$ kW, $g_{(l,3)} = 7$ kW, $g_{(l,2)} = 4$ kW, and $g_{(l,1)} = 0$ kW; and the initial state of the generator prior to the use is the best state 4. The transition intensities are set as $\lambda^l_{(2,1)} = 0.3/\text{month}$, $\lambda^l_{(3,1)} = 0.2/\text{month}$, $\lambda^l_{(3,2)} = 0.3/\text{month}$, $\lambda^l_{(4,1)} = 0.1/\text{month}$, $\lambda^l_{(4,2)} = 0.2/\text{month}$, $\lambda^l_{(4,3)} =$

TABLE VI
COMPARISON OF ESTIMATION ERRORS WITH 14 SAMPLES

Error	Prior distribution	Continuous inspection data	Discontinuous inspection data
$\lambda^{l}_{(2,1)}$	0.130	0.097	0.085
$\lambda^{l}_{(3,1)}$	0.130	0.094	0.134
$\lambda^{l}_{(3,2)}$	0.130	0.095	0.111
$\lambda^{l}_{(4,1)}$	0.170	0.051	0.058
$\lambda^{l}_{(4,2)}$	0.130	0.063	0.100
$\lambda^{l}_{(4,3)}$	0.130	0.086	0.082

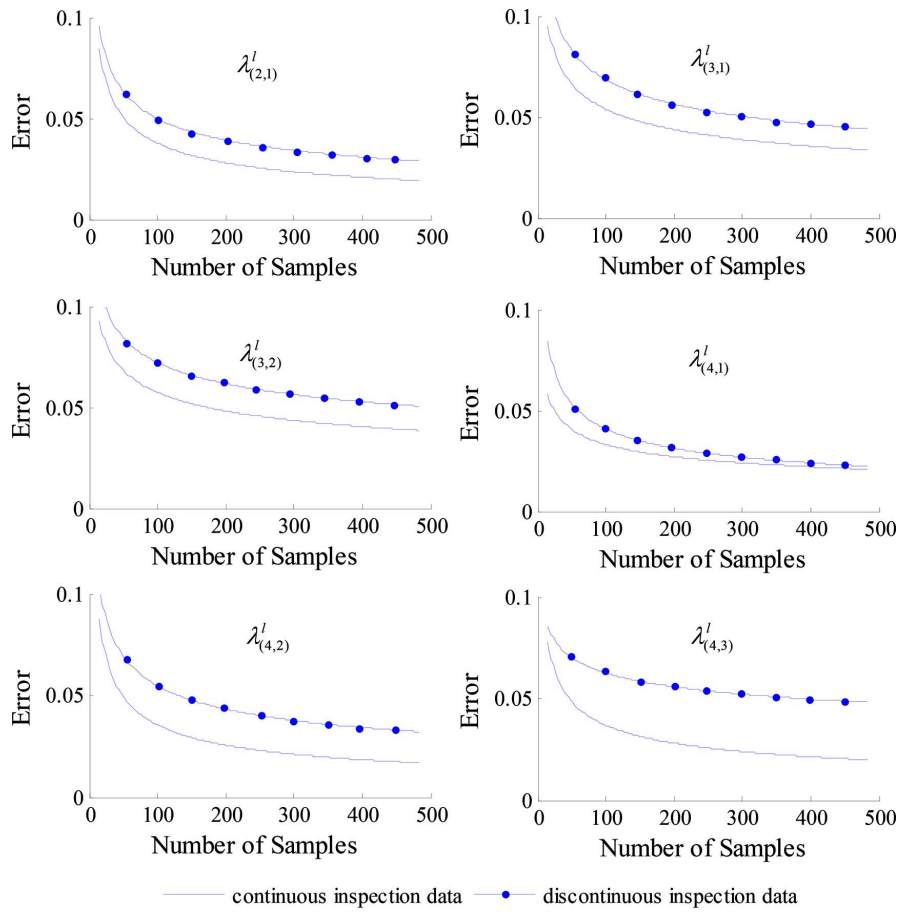

Fig. 5. Estimation errors with respect to the amount of observation data.

$0.3/\text{month}$, and they are estimated via the proposed method. We randomly generated 14 data sets emulating the actual observations (both continuously inspected, and discontinuously inspected) as shown in Table I, and Table III (respectively), corresponding to 14 samples (or realizations) of the studied generator. Ideally, by merging experts' prior knowledge with these actual observations, the estimated transition intensities should be close to the pre-set values which are used to generate the observed data given in Table I and Table III.

To construct the likelihood functions for the two types of data, the data in Table I and Table III are converted into Table II and Table IV. The likelihood function for the continuous inspection data can be obtained by plugging the observed data in Table II into (6), and the likelihood function for the discontinuous inspection data can be obtained by substituting the observed data in Table IV into (9). The prior of each transition intensity is assumed to be a uniform distribution with a range of $[0, 0.5]/\text{month}$, i.e., $\lambda^{l}_{(i,j)} \sim \text{Uniform}(0, 0.5)$. The Bayesian formula shown in (2) can be constructed by combining the likelihood function and the prior distribution. Because the posterior distribution is quite complicated, and no close form exists, the MCMC method is used to generate the posterior distribution via simulation.

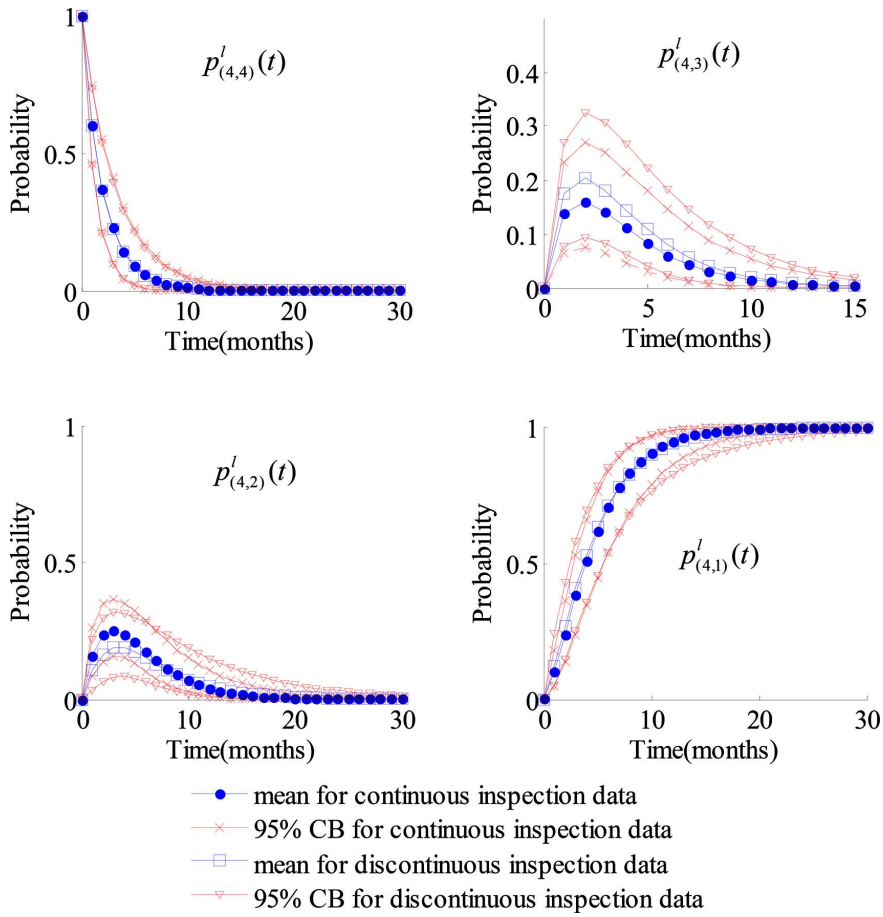

Fig. 6. Posterior state probabilities over time.

Fig. 4 plots the posterior distributions of $\boldsymbol{\lambda}^l$ computed from 5000 MCMC simulations after a burn-in period of 10,000 simulations. The true value of each transition intensity is indicated by a vertical solid line. As observed from Fig. 4, the estimates from the proposed Bayesian method encompass the true values of $\boldsymbol{\lambda}^l$. Table V summaries the statistic information of posterior distributions of $\boldsymbol{\lambda}^l$ for the continuous inspection data, and the discontinuous inspection data. As observed from Table V, the Bayesian estimation in both cases can effectively estimate the unknown parameters as most of the means of the estimated $\lambda^l_{(i,j)}$ are close to their true values. As seen in Fig. 4, if the amount of data sets increases to 100, the posterior distributions of $\boldsymbol{\lambda}^l$ are closer to the true values, and possess less uncertainty compared with the estimation by using 14 sets of observed data.

To compare the accuracy of the Bayesian estimation in the two cases, the estimation error is computed. Table VI gives the estimation error of $\boldsymbol{\lambda}^l$ for the continuous inspection data, and the discontinuous inspection data, and it is evaluated by

$$error = \int |\lambda^l_{(i,j)} - \hat{\lambda}^l_{(i,j)}| \cdot f^{post}(\lambda^l_{(i,j)}) d\lambda^l_{(i,j)}, \qquad (12)$$

where $\hat{\lambda}^l_{(i,j)}$ is the true value of $\lambda^l_{(i,j)}$. The results in Table VI illustrate that, compared to the prior distribution, the posterior distributions of estimated parameters are closer to the true values in most cases. In addition, the Bayesian estimation with the continuous inspection data is more accurate than that with the discontinuous inspection data.

Fig. 5 depicts the trend of estimation errors with the increase of observation data. For each data size, we use ten sets of randomly generated samples, and compute the average value of estimation errors. See that the estimation errors of both cases are approaching zero as the amount of data goes to infinity, indicating the proposed Bayesian estimation can achieve reasonable accuracy with sufficient observation data. The uncertainty associated with parameter estimation is also reduced by increasing the data. Additionally, it is also found that estimations from continuous inspection data always outperform that from discontinuous inspection data, regardless of the data size.

Given the posterior distributions of $\boldsymbol{\lambda}^l$, the posterior state probabilities of the studied component at any time instant t can be computed according to the simulation procedure introduced in Section IV. Fig. 6 plots the 95% confidence bounds, and the means of the posterior state probabilities for both cases. Fig. 7 delineates the posterior distributions of the state probabilities at $t = 5$ months for both continuous and discontinuous inspection data.

Note that the proposed Bayesian estimation method is also applicable to any components with more than four states. Nevertheless, the computational cost will increase due to two reasons. First, the number of Kolmogorov differential equations in

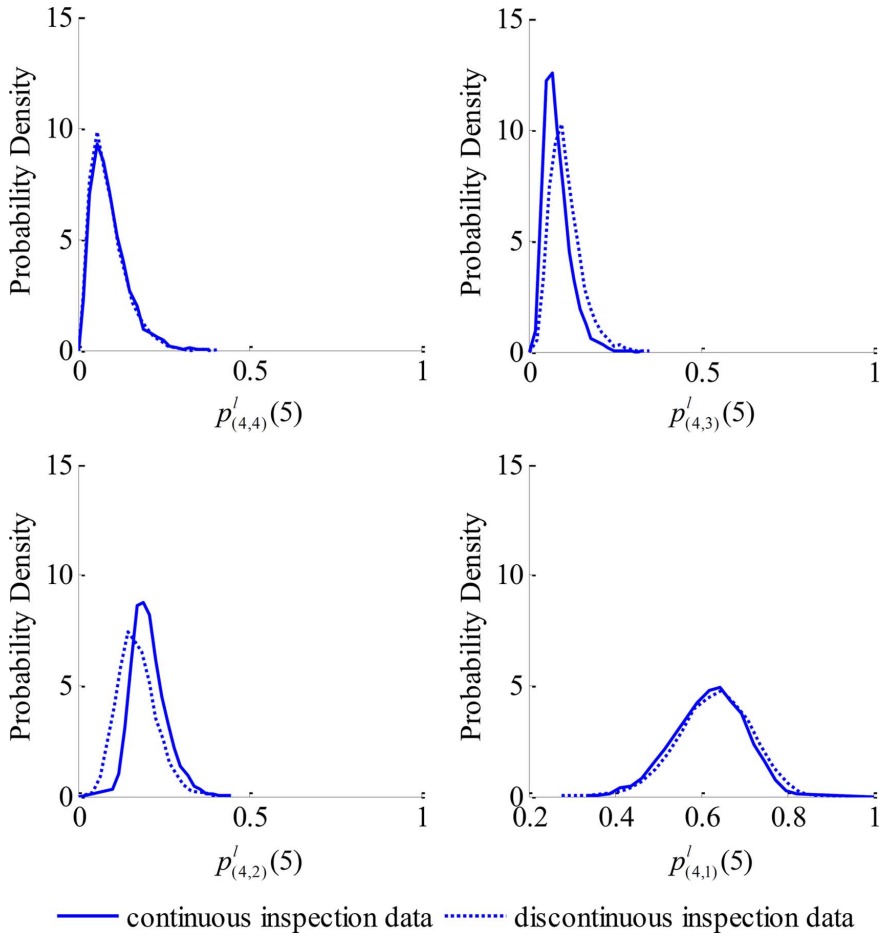

Fig. 7. The posterior state distributions at $t = 5$ months.

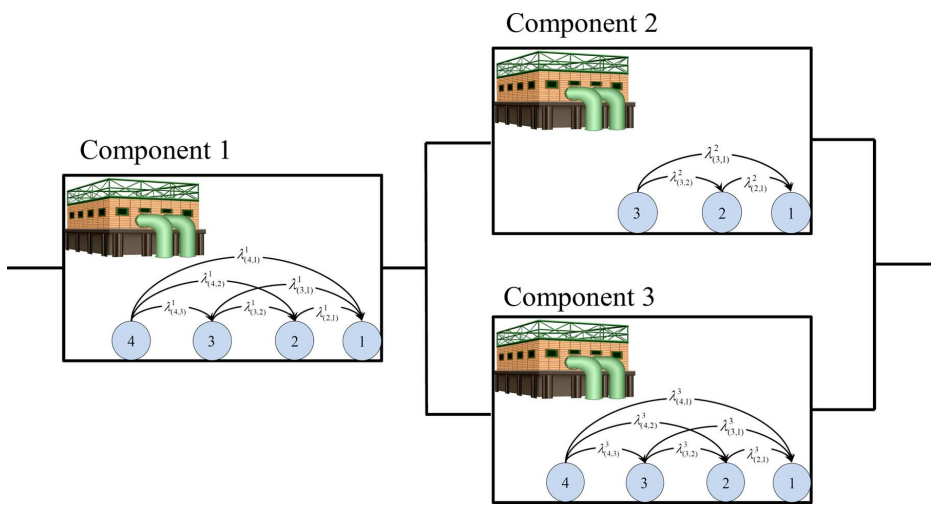

Fig. 8. The structure of the studied multi-state power generating system.

(1) which are used to calculate component state probabilities as a function of transition intensities equals k_l, the total number of states of a multi-state component l. The complexity of the likelihood functions, i.e., (6) and (9), will also increase with respect to k_l because the number of the possible outcomes of the multinomial distribution in (6) and (9) increases. Second, the number of transition intensities to be estimated will be increased to $(k_l - 1)k_l/2$ if a higher state can transit to any lower states. Consequently, the number of samplings in each simulation iteration of the MCMC method will increase to $(k_l - 1)k_l/2$.

B. A Power Generating System

A multi-state power generating system consisting of three multi-state power units is shown in Fig. 8.

TABLE VII
DISCONTINUOUS INSPECTION DATA OF 14 SAMPLES FOR COMPONENT #1

State i observed in the last inspection	Inspection interval $\Delta t_1 = 2$ months				
	State j observed in adjacent inspection				
		$j=4$	$j=3$	$j=2$	$j=1$
	$m_i^{\Delta t_1}$	$m_{(i,4)}^{\Delta t_1}$	$m_{(i,3)}^{\Delta t_1}$	$m_{(i,2)}^{\Delta t_1}$	$m_{(i,1)}^{\Delta t_1}$
$i=4$	19	11	4	3	1
$i=3$	11	—	7	1	3
$i=2$	10	—	—	6	4
State i observed in the last inspection	Inspection interval $\Delta t_2 = 4$ months				
	State j observed in adjacent inspection				
		$j=4$	$j=3$	$j=2$	$j=1$
	$m_i^{\Delta t_2}$	$m_{(i,4)}^{\Delta t_2}$	$m_{(i,3)}^{\Delta t_2}$	$m_{(i,2)}^{\Delta t_2}$	$m_{(i,1)}^{\Delta t_2}$
$i=4$	9	3	1	4	1
$i=3$	3	—	2	1	0
$i=2$	21	—	—	16	5

TABLE VIII
CONTINUOUS INSPECTION DATA OF 14 SAMPLES FOR COMPONENT #2

Initial state i of a transition	Total sojourning time(months) T_i	Total number m_i	Destination state j of a transition	
			$j=2$	$j=1$
			$m_{(i,2)}$	$m_{(i,1)}$
$i=3$	55.11	14	10	4
$i=2$	49.94	10	—	10

Component #1 has four possible performance capacities: $g_{(1,4)} = 12$ kW, $g_{(1,3)} = 8$ kW, $g_{(1,2)} = 4$ kW, and $g_{(1,1)} = 0$ kW. And it is discontinuously inspected every 2 or 4 months. The corresponding inspection data collected from 14 samples are tabulated in Table VII based the proposed formats. Component #2 has three possible performance capacities: $g_{(2,3)} = 8$ kW, $g_{(2,2)} = 5$ kW, and $g_{(2,1)} = 0$ kW. And it is continuously inspected. The exact transition times from 14 samples are recorded in Table VIII. Component #3 is the multi-state generator as studied earlier in Section V-A. The system performance capacity at any time instant is equal to $\min\{G_1(t), G_2(t) + G_3(t)\}$.

By substituting the collected data into (6) or (9), the likelihood function of each individual component can be obtained. The prior of each transition intensity is also assumed to be a uniform distribution with a range of $[0, 0.5]/\text{month}$. In the same manner with Section V-A, the posterior distribution of transition intensities of components 1 and 2 can be derived with the assistance of WinBUGS software.

By using the UGF, the number of distinct performance capacities of the entire system can be identified, corresponding to the number of system states. The studied system has eight distinct performance capacities, i.e., $\mathbf{g}_s = \{g_1 = 0, g_2 = 4, g_3 = 5, g_4 = 7, g_5 = 8, g_6 = 9, g_7 = 10, g_8 = 12\}$ kW. Following the procedure introduced in Section IV, the posterior system state probabilities can be evaluated by substituting the random samples generated from the posterior distributions of the transition intensities of the three components into the corresponding UGFs. Fig. 9 plots the mean, and 95% confidence bounds of the posterior system state probabilities with respect to time t. To compute the posterior distributions of system state probabilities at any time instant t, the proposed simulation method takes 0.042 seconds via Matlab 2012 on a PC with an Intel Core i5 2.27 GHz CPU and 2.0 GB RAM when N_{sa} is set to 5000.

TABLE IX
USER DEMAND LEVELS

User demand	3 kW	5 kW	7 kW
Probability	0.4	0.3	0.3

The possible values and the corresponding probabilities of user demand are given in Table IX. Hence, the system reliability at any time instant t can be evaluated via (10), and its mean value and the 95% confidence bounds are shown in Fig. 10. In the same manner, by using (11), the mean and the 95% confidence bounds of the instantaneous expected performance capacity are also obtained, and shown in Fig. 11.

As exemplified in Section V-A, adding more observation data will reduce estimation uncertainty. However, each component in the MSS may have a different contribution to the reliability estimation uncertainty of the entire system. To demonstrate this point, we increase the amount of observation data from 14 to

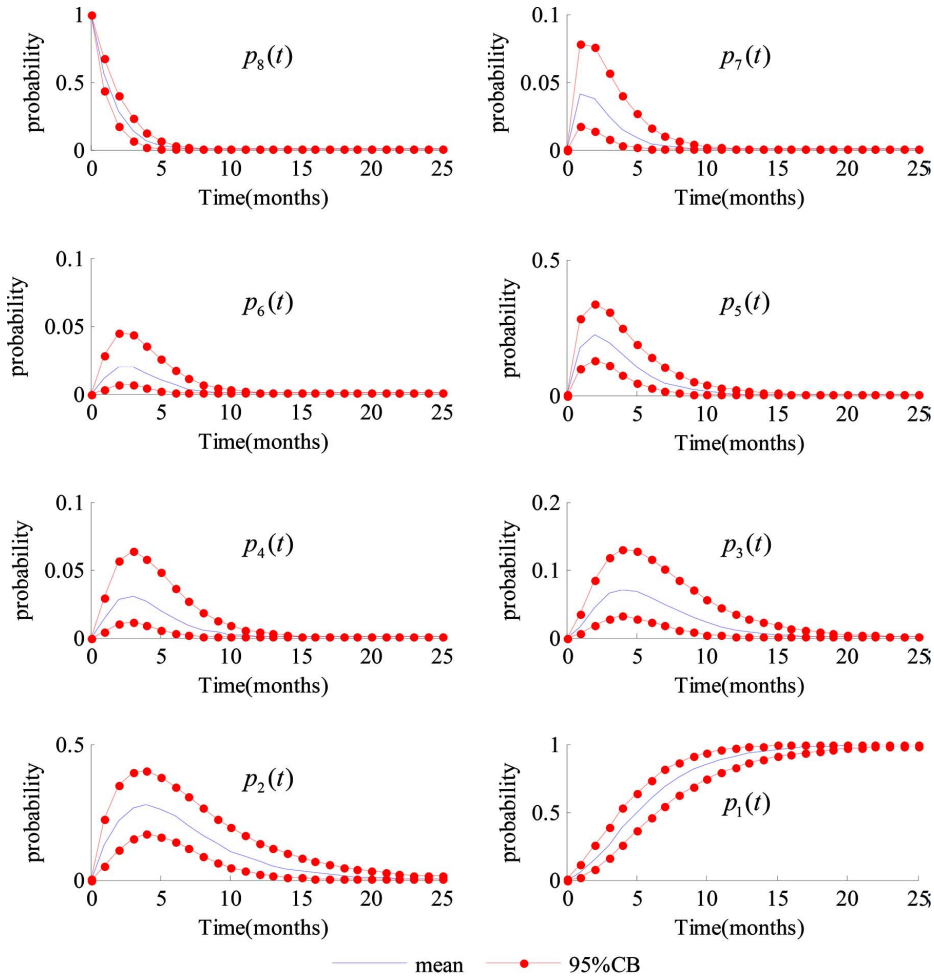

Fig. 9. The posterior system state probabilities over time.

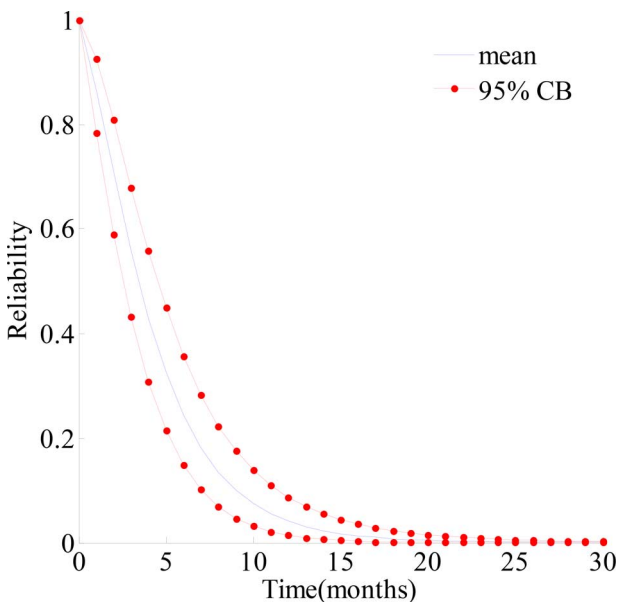

Fig. 10. The reliability of the entire MSS.

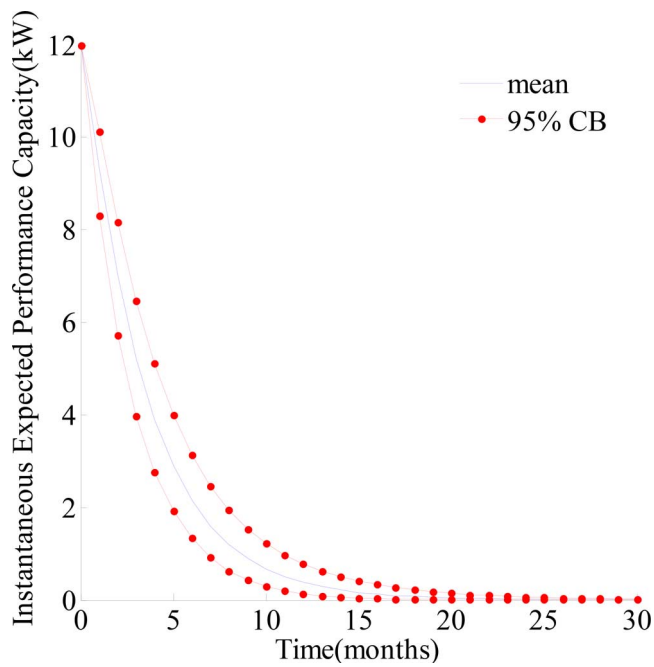

Fig. 11. The instantaneous expected performance capacity.

100 for one of three components, and compare the uncertainty reduction of system reliability estimation resulting from the improvement of parameter estimation of each component. Fig. 12 plots the mean and 95% confidence bounds of the estimated system reliability before, and after adding observation data. It

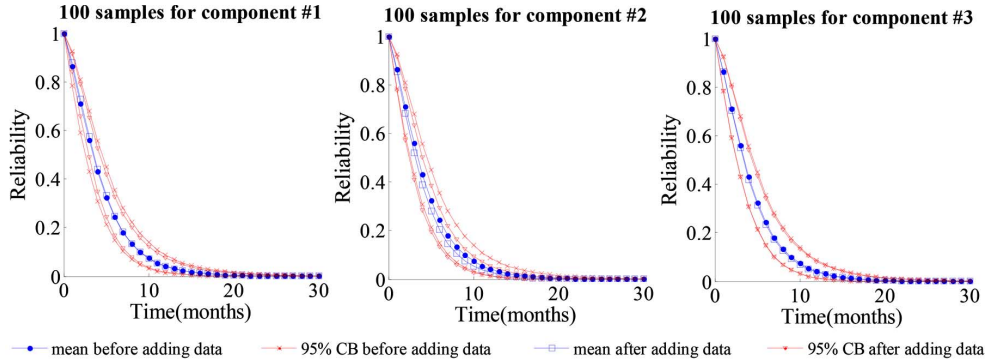

Fig. 12. The system reliability before and after adding observation data.

TABLE X
THE STANDARD DEVIATION OF SYSTEM RELIABILITY WITH 100 SAMPLES OF EACH COMPONENT COMPARED TO THE INITIAL DATA

Time(months)	Standard deviation			
	Initial data	100 samples for component #1	100 samples for component #2	100 samples for component #3
t=1.0	0.0364	**0.0188**	0.0358	0.0358
t=2.0	0.0557	**0.0355**	0.0534	0.0540
t=3.0	0.0633	**0.0427**	0.0579	0.0592
t=5.0	0.0591	**0.0450**	0.0483	0.0545
t=8.0	0.0390	0.0315	**0.0269**	0.0361
t=10.0	0.0274	0.0224	**0.0171**	0.0254
t=15.0	0.0103	0.0086	**0.0054**	0.0097
t=20.0	0.0038	0.0032	**0.0018**	0.0036

is observed that the uncertainty of reliability estimation can be significantly reduced by adding the observation data for component #1 or component #2. Such a reduction is not obvious in the case of increasing the data for component #3. The standard deviations of the estimated reliability at several time instants are presented in Table X, and the smallest standard deviations (indicating the least amount of uncertainty) among four cases are highlighted. As seen in Table X, compared with other cases, adding observation data for component #1 leads to a greater amount of uncertainty reduction at the very beginning stage (i.e., $0 \sim 5$ months). Nevertheless, it becomes more effective in term of uncertainty reduction at the later stage (i.e., $5 \sim 20$ months) by collecting additional data for component #2. Compared to the previous two cases, the uncertainty reduction by increasing the data of component #3 is always inferior.

VI. CONCLUSIONS, AND REMARKS

In this paper, a Bayesian framework is developed to assess the reliability and performance of multi-state systems consisting of multi-state components. The transition intensities that characterize the deterioration process of multi-state components are estimated by synthesizing experts' prior knowledge and observation data. The likelihood functions for both continuous and discontinuous inspection data are derived. A simulation method embedded with the UGF is developed to compute the posterior component state probabilities, system state probabilities, reliability function, and instantaneous expected performance capacity. Our numerical experiments show that the proposed Bayesian estimation can effectively estimate the unknown parameters, and assess the reliability and performance of MSSs via the posterior distributions of transition intensities.

It is worth mentioning that there are still some challenges to be addressed in our future work. First, the Bayesian estimation can be extended to more general cases by integrating non-homogenous continuous-time Markov models and semi-Markov models. Second, allocating resources to reduce the uncertainty of reliability estimation will be studied based on the current work. Finally, the Bayesian estimation by combining observation data with a hierarchical relation will be investigated in our future work.

APPENDIX

The WinBUGS scripts for estimating transition intensities of a three-state component with continuous inspection data.

model{
# **Model Construction**
for (i in 2:3){ *#transitions from states 2 and 3*
#specify the Poisson distribution for the total number of transitions 'totalm[i]'
totalm[i] ~ dpois(poispar[i])
#parameter 'poispar[i]' for the Poisson distribution
poispar[i] < -leavelambda[i]*totalt[i]
#intensity of leaving state i 'leavelambda[i]'
#and total time sojourning at state i 'totalt[i]'
}
#specify the multinomial distribution for the numbers of
#transitions from state 3 to states 1 and 2'
$m[3, 1:2]$
'

```
    m[3, 1 : 2] ~ dmulti(q3[1 : 2], totalm[3])
  leavelambda[2] < -lambda21
#transition intensity from state 2 to state 1 'lambda21'
    leavelambda[3] < -lambda31 + lambda32
#transition intensity from state 3 to state 1 'lambda31'
#and transition intensity from state 3 to state 2 'lambda32'
  q3[1] < -lambda31/leavelambda[3]
#conditional probability that
#transition is from state 3 to state 1'
  q3[1]
,
  q3[2] < -lambda32/leavelambda[3]
#conditional probability that
#transition is from state 3 to state 2 '
  q3[2]
,
# Prior Specification
    lambda32 ~ dunif(0, .5); lambda31 ~ dunif(0, .5);lambda21 ~ dunif(0, .5)
#prior distributions (uniform distributions)
  }
```

The WinBUGS scripts for estimating transition intensities of a three-state component with discontinuous inspection data.

```
model{
# Model Construction
#specify the multinomial distribution for the numbers of
#transitions from state i to states 1, 2 and 3 'm[i,1:3]'
    for(i in1 : 3){m[i, 1 : 3] ~ dmulti(p[i, 1 : 3], totalm[i])}
#expression of component state probability at state j given the
initial state i 'p[i,j]'
    p[1, 1] < −1
    p[1, 2] < −0
    p[1, 3] < −0
    p[2, 1] < −1- exp(-lambda21*deltat)
#transition intensity from state 2 to state 1 'lambda21'
#and inspection interval 'deltat'
    p[2, 2] < - exp(-lambda21*deltat)
    p[2, 3] < −0
    p[3, 1] < - < -(exp(-deltat*(lambda31 + lambda32))*(lambda21 − lambda31))/(lambda31
    −lambda21 + lambda32) −
(lambda32*exp(−lambda21*deltat))/(lambda31
    −lambda21 + lambda32) + 1
#transition intensity from state 3 to state 1 'lambda31'
#and transition intensity from state 3 to state 2 'lambda32'
    p[3, 2] < - -(lambda32*(exp(−deltat*(lambda31 + lambda32))
    − exp(−lambda21*deltat)
))
  /(lambda31 − lambda21 + lambda32)
    p[3, 3] < − exp(−deltat*(lambda31 + lambda32))
# Prior Specification
    lambda32 ~ dunif(0, .5); lambda31 ~ dunif(0, .5)
;
  lambda21 ~ dunif(0, .5)
#prior distributions (uniform distributions)
  }
```

REFERENCES

[1] W. Kuo and M. J. Zuo, *Optimal Reliability Modeling: Principles and Applications*. Hoboken, NJ, USA: Wiley, 2003.

[2] A. Lisnianski and G. Levitin, *Multi-State System Reliability Assessment, Optimization, Application*. Singapore: World Scientific, 2003.

[3] M. Nourelfath, M. C. Fitouhi, and M. Machani, "An integrated model for production and preventive maintenance planning in multi-state systems," *IEEE Trans. Rel.*, vol. 59, no. 3, pp. 496–506, 2010.

[4] D. Elmakias, *New Computational Methods in Power System Reliability*. London, U.K.: Springer, 2008.

[5] J. E. Ramirez-Marquez and D. W. Coit, "A Monte-Carlo simulation approach for approximating multi-state two-terminal reliability," *Rel. Eng. Syst. Safety*, vol. 87, no. 2, pp. 253–264, 2005.

[6] Y. Ding, M. J. Zuo, Z. Tian, and W. Li, "The hierarchical weighted multi-state k-out-of-n system model and its application for infrastructure management," *IEEE Trans. Rel.*, vol. 59, no. 3, pp. 593–603, 2010.

[7] A. Shrestha and L. Xing, "A logarithmic binary decision diagram-based method for multistate system analysis," *IEEE Trans. Rel.*, vol. 57, no. 4, pp. 595–606, 2008.

[8] A. Lisnianski, "Extended block diagram method for a multi-state system reliability assessment," *Rel. Eng. Syst. Safety*, vol. 92, no. 12, pp. 1601–1607, 2007.

[9] G. Levitin, *The Universal Generating Function in Reliability Anal. and Optimization*. London, U.K.: Springer, 2005.

[10] W. Li and M. J. Zuo, "Reliability evaluation of multi-state weighted k-out-of-n systems," *Rel. Eng. Syst. Safety*, vol. 93, no. 1, pp. 160–167, 2008.

[11] Y. Liu and H. Z. Huang, "Reliability assessment for fuzzy multi-state systems," *Int. J. Syst. Sci.*, vol. 41, no. 4, pp. 365–379, 2010.

[12] Y. Liu, H. Z. Huang, and G. Levitin, "Reliability and performance assessment for fuzzy multi-state element," *J. Risk Rel.*, vol. 222, no. 4, pp. 675–686, 2008.

[13] A. Lisnianski, I. Frenkel, and Y. Ding, *Multi-State System Reliability Analysis and Optimization for Engineers and Industrial Managers*. London, U.K.: Springer, 2010.

[14] A. Lisnianski, D. Elmakias, D. Laredo, and H. B. Haim, "A multi-state Markov model for a short-term reliability analysis of a power generating unit," *Rel. Eng. Syst. Safety*, vol. 98, no. 1, pp. 1–6, 2012.

[15] Y. Ding, M. J. Zuo, A. Lisnianski, and Z. Tian, "Fuzzy multi-state systems: general definitions, and performance assessment," *IEEE Trans. Rel.*, vol. 57, no. 4, pp. 589–594, 2008.

[16] C. Y. Li, X. Chen, X. S. Yi, and J. Y. Tao, "Interval-valued reliability analysis of multi-state systems," *IEEE Trans. Rel.*, vol. 60, no. 4, pp. 595–606, 2011.

[17] S. Destercke and M. Sallak, "An extension of universal generating function in multi-state systems considering epistemic uncertainties," *IEEE Trans. Rel.*, vol. 62, no. 2, pp. 504–514, 2013.

[18] P. Wang, B. D. Youn, Z. Xi, and A. Kloess, "Bayesian reliability analysis with evolving, insufficient, and subjective data sets Article ID 111008," *J. Mech. Design-Trans. ASME*, vol. 131, no. 11, 2009.

[19] Y. Liu, Y. Li, H. Z. Huang, M. J. Zuo, and Z. Sun, "Optimal preventive maintenance policy under fuzzy Bayesian reliability," *IIE Trans.*, vol. 42, no. 10, pp. 734–745, 2010.

[20] M. S. Hamada, A. G. Wilson, C. S. Reese, and H. F. Martz, *Bayesian Reliability*. London, U.K.: Springer, 2008.

[21] D. Kelly and C. Smith, *Bayesian Inference for Probabilistic Risk Assessment*. London, U.K.: Springer, 2011.

[22] A. Lisnianski, I. Frenkel, and Y. Ding, *Multi-State System Reliability Analysis and Optimization for Engineers and Industrial Managers*. London, U.K.: Springer, 2010.

[23] J. Q. Smith, *Decision Analysis: A Bayesian Approach*. London, U.K.: Chapman and Hall, 1998.

[24] N. J. Welton and A. E. Ades, "Estimation of Markov chain transition probabilities and rates from fully and partially observed data: uncertainty propagation, evidence synthesis, and model calibration," *Med. Decision Making*, vol. 25, no. 6, pp. 633–745, 2005.

[25] I. Ntzoufras, *Bayesian Modeling Using WinBUGS*. Hoboken, NJ, USA: Wiley, 2009.

[26] T. Jin and D. W. Coit, "Variance of system-reliability estimates with arbitrarily repeated components," *IEEE Trans. Rel.*, vol. 50, no. 4, pp. 409–413, 2001.

Yu Liu (M'14) is a Professor in the School of Mechanical, Electronic, and Industrial Engineering, at the University of Electronic Science and Technology of China. He received his PhD degree in Mechatronics Engineering from the University of Electronic Science and Technology of China.

He was a Visiting Pre-doctoral Fellow in the Department of Mechanical Engineering at Northwestern University, USA from 2008 to 2010 and a Postdoctoral Research Fellow in the Department of Mechanical Engineering, at the University of Alberta, Canada from 2012 to 2013. He has published over 50 peer-reviewed papers in international journals and conferences. His research interests include system reliability modeling and analysis, maintenance decisions, prognostics and health management, and design under uncertainty.

Peng Lin received his bachelor degree in Industrial Engineering from the School of Mechanical, Electronic, and Industrial Engineering, at the University of Electronic Science and Technology of China in 2014. He is currently pursuing his doctoral degree in Department of Industrial and Manufacturing Systems Engineering, at the University of Hong Kong.

He was an Undergraduate Research Assistant for Dr. Y. Liu during 2012–2014. His research interests include Bayesian reliability assessment, and production scheduling.

Yan-Feng Li received his PhD degree in Mechatronics Engineering from the University of Electronic Science and Technology of China in 2013.

He is a lecturer in the School of Mechanical, Electronic, and Industrial Engineering, at the University of Electronic Science and Technology of China. His research interests include reliability analysis and evaluation of complex systems, dynamic fault tree modelling, Bayesian networks modelling, and probabilistic inference.

Hong-Zhong Huang (M'06) received a PhD degree in Reliability Engineering from Shanghai Jiaotong University, China

He is a Professor of the School of Mechanical, Electronic, and Industrial Engineering at the University of Electronic Science and Technology of China. He has held visiting appointments at several universities in the USA, Canada, and Asia. He has published 200 journal papers and 5 books in the fields of reliability engineering, optimization design, fuzzy sets theory, and product development. His current research interests include system reliability analysis, warranty, maintenance planning and optimization, and computational intelligence in product design.

Prof. Huang is an ISEAM Fellow, a technical committee member of ESRA, a Co-Editor-in-Chief of the *International Journal of Reliability and Applications*, and an Editorial Board Member of several international journals. He received the William A. J. Golomski Award from the Institute of Industrial Engineers in 2006, and the Best Paper Award of the ICFDM2008, ICMR2011, and QR2MSE2013.